01 Jan 1968

# Age Hardening In A Mg-9 Wt.% Al Alloy

J. Beverley Clark
*Missouri University of Science and Technology*

## Recommended Citation

J. B. Clark, "Age Hardening In A Mg-9 Wt.% Al Alloy," *Acta Metallurgica*, vol. 16, no. 2, pp. 141 - 152, Elsevier, Jan 1968.
The definitive version is available at https://doi.org/10.1016/0001-6160(68)90109-0

# AGE HARDENING IN A Mg–9 WT.% Al ALLOY*

J. B. CLARK†

The precipitation process and age hardening mechanism in a Mg–9 wt.% Al alloy were studied principally by transmission electron microscopy. This alloy age hardens by the general precipitation of plates of the equilibrium $Mg_{17}Al_{12}$ phase on the basal plane of the magnesium solid solution matrix. No evidence for the formation of either G.P. zones or a transition lattice of the $Mg_{17}Al_{12}$ precipitate was obtained. Cellular precipitation occurs competitively with the general precipitation at nearly all age hardening temperatures. In the solution treated condition, basal slip and $\{10\bar{1}2\}$ twins are the principal deformation modes. Precipitation induces cross slip on the prism planes and tends to suppress $\{10\bar{1}2\}$ twin formation. The alloys are hardened by complex dislocation tangles formed by the interaction of slip dislocations on the prism and basal planes. Neither slip dislocations nor $\{10\bar{1}2\}$ twins shear the $Mg_{17}Al_{12}$ plates.

## DURCISSEMENT APRES VIEILLISSEMENT DANS UN ALLIAGE Mg–9% PDS Al

On étudie, principalement par microscopie électronique en transmission, le processus de précipitation et le mécanisme de durcissement après vieillissement dans un alliage Mg–9% en poids Al. Le durcissement de cet alliage se fait par la précipitation générale de disques de la phase d'équilibre $Mg_{17}Al_{12}$ sur le plan de base de la matrice de la solution solide de magnésium. On n'obtient aucune preuve de la formation soit de zones de G.P. soit d'un réseau de transition du précipité de $Mg_{17}Al_{12}$. La précipitation cellulaire entre en compétition avec la précipitation générale à presque toutes les températures de durcissement après vieillissement. Dans le cas de traitement en solution les principaux modes de déformation sont le glissement de base et les macles $\{10\bar{1}2\}$. La précipitation entraîne la déviation sur les plans prismatiques et tend à supprimer la formation de macles $\{10\bar{1}2\}$. Le purcissement des alliages est dû à un enchevêtrement complexe de dislocations formé par l'interaction de dislocations de glissement sur les plans prismatiques et le plan de base. Ni les dislocations de glissement ni les macles $\{10\bar{1}2\}$ ne cisaillent les disques de $Mg_{17}Al_{12}$.

## AUSHÄRTUNG IN EINER Mg–9 GEW.-% A.-LEGIERUNG

Mittels elektronenmikroskopischer Durchstrahlung wurde der Ausscheidungsprozess und die Aushärtung in einer Mg–9 Gew.-% Al-Legierung untersucht. Diese Legierung härtet durch Ausscheidung von Plättchen der $Mg_{17}Al_{12}$-Gleichgewichtsphase auf der Basisebene der Magnesiummatrix. Es wurden keine Hinweise für die Bildung von G.P. Zonen oder ein Übergangsgitter der $Mg_{17}Al_{12}$-Ausscheidung gefunden. Zellularausscheidung steht bei fast allen Alterungstemperaturen im Wettbewerb mit der allgemeinen Ausscheidung. Im Lösungsfalle sind Basisgleitung und $\{10\bar{1}2\}$-Zwillinge die vorherrschenden Verformungsmechanismen. Die Ausscheidung induziert Quergleitung auf den prismatischen Ebenen und neigt zur Unterdrückung der $\{10\bar{1}2\}$ Zwillingsbildung. Die Legierungen werden gehärtet durch komplexe Versetzungsknäuel, die durch Wechselwirkung von Gleitversetzungen auf Prismen- und Basisebene entstehen. Die $Mg_{17}Al_{12}$-Plättchen werden weder durch Gleitversetzungen noch durch $\{10\bar{1}2\}$-Zwillinge geschert.

## INTRODUCTION

In contrast to the extensive knowledge of precipitation processes and age hardening mechanisms in face centered cubic alloys, little is known concerning these processes in hexagonal close packed alloys. In an effort to gain more insight into these mechanisms, age hardening studies on a series of magnesium alloys are in progress. In the first investigation conducted on a Mg–5 wt.% Zn alloy,(1) it was shown that the hardening precipitate was a transition lattice of the MgZn phase which forms in long thin rods perpendicular to the basal plane. Although these precipitate rods are oriented efficiently to block basal slip, the solubility of zinc in magnesium is too low and the size of the individual precipitates is too large to produce a sufficiently small inter-particle spacing. Consequently, the age hardening response of this Mg–Zn alloy is small—less than a factor of two. In Mg–Al alloys, however, the maximum solubility is 12.7 wt.% Al, as compared with 8.1 wt.% Zn. Also the densities of the matrix and precipitate are nearly equal whereas in the Mg–Zn system, the much higher density of the precipitate results in a smaller volume of precipitate, further compounding the effect of a lower solubility. Therefore, solely on the basis of the total volume fraction of available precipitate, the age hardening of Mg–Al alloys should be greater than that of Mg–Zn alloys. As illustrated in Fig. 1, however, in which the optimum age hardening curve of a Mg–9 wt.% Al alloy is compared with that of a Mg–5 wt.% Zn alloy, this is not the case. This investigation was accordingly undertaken to determine whether the poor age hardening response of the Mg–Al alloys is due to some aspect of the precipitation

---

* Received June 6, 1967.

† Now at: Department of Metallurgical Engineering, University of Missouri, Rolla, Missouri. This work was done at the Scientific Laboratory, Ford Motor Company, Dearborn, Michigan.

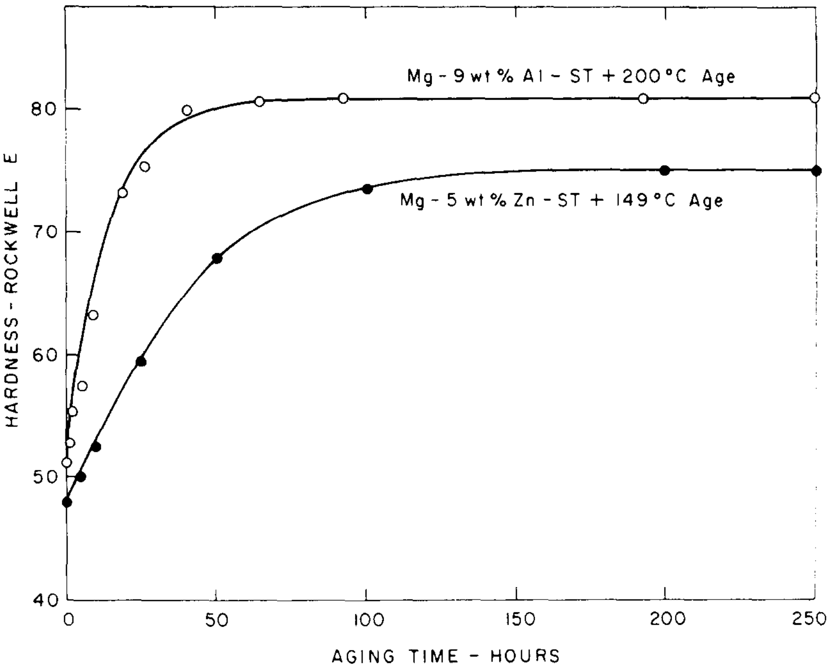

FIG. 1. Comparison of the optimum age hardening curves of a Mg–9 wt.% Al alloy and a Mg–5 wt.% Zn alloy.

process (particle size, shape, etc.) or to the nature of the interaction of the deformation processes with the precipitates.

The precipitation processes in Mg–Al alloys have been previously studied(2–4) principally by light microscopy and X-ray diffraction. Within the limitations of these methods, it was determined that precipitation in this system is relatively simple; plates of the equilibrium phase, $Mg_{17}Al_{12}$, are formed without the intervention of a transition phase. No evidence of G.P. zones was reported; such structures, however, would be difficult to detect in these alloys because of the proximity of the atomic scattering factors of aluminum and magnesium. Talbot and Norton(2) found that the hardness maximum was reached when X-ray evidence showed less than 50% completion of precipitation. Similar results were found by Leontis and Nelson(5) in Mg–Al alloys with small amounts of zinc. These results would seem to indicate that the poor age hardening of these alloys is related to the nature of the dislocation–precipitate interaction rather than limitations in solute solubility as in Mg–Zn alloys. In the Mg–Al system there is more than enough precipitate available, but the precipitate dispersion is ineffective in strengthening these alloys.

Murakami *et al.*(6) used transmission electron microscopy to confirm this previously reported precipitation process in a Mg–11.6 wt.% Al alloy, but the details of the process and the cause of the poor age hardening response were not investigated.

In the present investigation, the Mg–9 wt.% Al alloy was selected for study because this composition is fairly easy to homogenize after casting and yet offers a wide temperature range for precipitation.

## EXPERIMENTAL PROCEDURE

Bar stock ($\frac{1}{4}$ in. × $1\frac{1}{2}$ in. in cross section) and foil (0.01 in. thick) of Mg–9 wt.% Al were obtained through the courtesy of S. L. Couling of the Dow Metal Products Company. The alloy was prepared from singly sublimed magnesium and high purity aluminum using standard melting and alloying procedures.

Bar and foil specimens were solution annealed under argon for 1 hr at 540°C and then quenched in water. Age hardening treatments at 150, 175, 200 and 260°C were conducted in air furnaces and terminated by a water quench.

The window method was used to thin the foils for examination in the electron microscope. Specimens in the solution treated condition or with small amounts of precipitate were chemically thinned in a solution of 1 volume of concentrated $HNO_3$ plus 2 volumes methyl alcohol.(7) However, since the nitric acid in this thinning solution tends to dissolve the $Mg_{17}Al_{12}$ precipitate, specimens with larger amounts of precipitate were thinned in a hot phosphoric acid solution and then cleaned with a special rinse (see Appendix). Conversely the phosphoric acid thinning solution cannot be used on specimens containing too little precipitate, since it produces artifacts in the magnesium solid solution regions of the specimen under these circumstances. These artifacts which resemble somewhat dislocation loops can obscure the true microstructure. Portions of the thinned foils were examined in a Philips 200 electron microscope operating at 100 kV.

Hardness as a function of aging time was measured on a Rockwell machine using the E scale. Each reported value is the average of at least three measurements having a maximum spread of ±2 points. Tensile strengths as a function of heat treatments and testing temperature were measured on an Instron machine equipped with a tensile attachment capable of testing over the temperature range of −196°C to 300°C.

For trace analysis of the deformation processes in these alloys as a function of age hardening and test temperature, large grained specimens of the alloys were grown by the strain–anneal method. The surface of these large grained specimens were polished at room temperature in a 50% phosphoric acid–50% ethyl alcohol solution. Before polishing, all specimens were solution treated because the polishing solution tended to attack aged specimens. Polished specimens were encapsulated in Pyrex vials under an equivalent atmosphere of argon and given the required precipitation treatments. As shown in Fig. 14, a slight loss of polish, due to vaporization of magnesium occurred during aging but the surface of the aged specimens was satisfactory for subsequent slip trace analysis. The orientation of selected grains of the heat treated specimens was determined by the Laue back reflection method using cobalt radiation. The specimens were then compressed 4% and the deformation processes were identified on the basis of a one-surface trace analysis.

## RESULTS

### *Age hardening*

The age hardening curves for Mg–9 wt.% Al alloy at a variety of temperatures are shown in Fig. 2. The configuration of these curves follows the classical age hardening pattern. Aging at temperatures between 150° and 200°C produces the same maximum hardness. The 150° curve merges with the 175 and 200°C curves at 450 hr. As in previous studies,(2,4) overaging was not observed at any of these aging temperatures. Tensile tests on a series of aged test bars indicated that the hardness of the alloy varied proportionately with the tensile yield strength of the alloy.

### *Precipitation processes*

In Mg–Al alloys, both general (intragranular) and cellular (discontinuous) precipitation occur competitively throughout the range of age-hardening temperatures studied. First let us consider the general precipitation process.

(a) *General or intragranular precipitation.* The general results of previous studies(2–6) were confirmed. The only precipitate is non-coherent plates of the equilibrium $Mg_{17}Al_{12}$ phase. No indications of a transition lattice form of $Mg_{17}Al_{12}$ or G.P. zone formation were seen, even at low temperatures, or

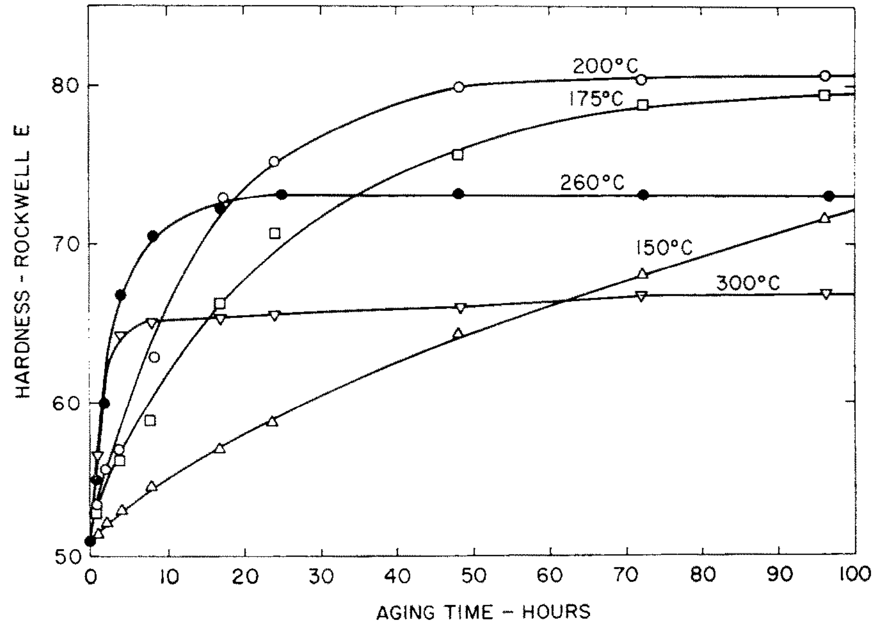

FIG. 2. Age hardening of a Mg–9 wt.% Al alloy as a function of aging temperature.

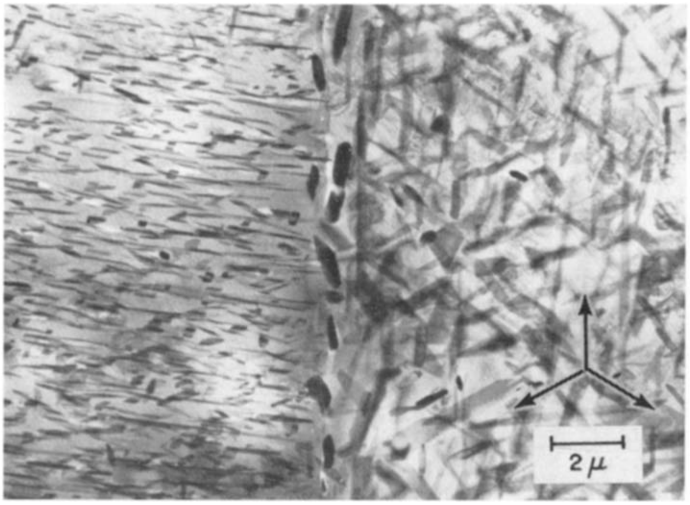

FIG. 3. Plates of the equilibrium $Mg_{17}Al_{12}$ phase with basal plane habit. In the left grain, the plane of the foil is near $(10\bar{1}1)$; in the right grain, near (0001). Arrows denote $[11\bar{2}0]$ directions. Alloy sample was aged 8 hr at 260°C.

during the early stages of precipitation. As shown in Fig. 3, the $Mg_{17}Al_{12}$ plates form parallel to the basal plane and are elongated in the three close packed directions of the matrix. The basal habit plane and the plate morphology are shown more clearly in Fig. 4 in which the plane of the foil is nearly parallel to a prism plane of the matrix. This figure shows that even at this lower aging temperature (175°C) which produced nearly the highest level of hardness obtained, the inter-plate spacing is relatively large—about 2000 Å.

The well defined plate morphology indicates that a definite orientation relationship must exist between the $Mg_{17}Al_{12}$ plates and the magnesium solid solution matrix. The maintenance of the plate shape to large sizes, and after prolonged aging, indicates that broad faces of the plates must have a sessile dislocation structure whereas the edges of the plates probably have either a glissile dislocation or a disordered structure.(8,9) Unfortunately the orientation relationship of the structure of the $Mg_{17}$ $Al_{12}$ plates with the matrix could not be determined unambiguously by electron diffraction.

No coherency strains were observed around the precipitate. However, in hot stage experiments in which solution treated thin foil specimens were aged in

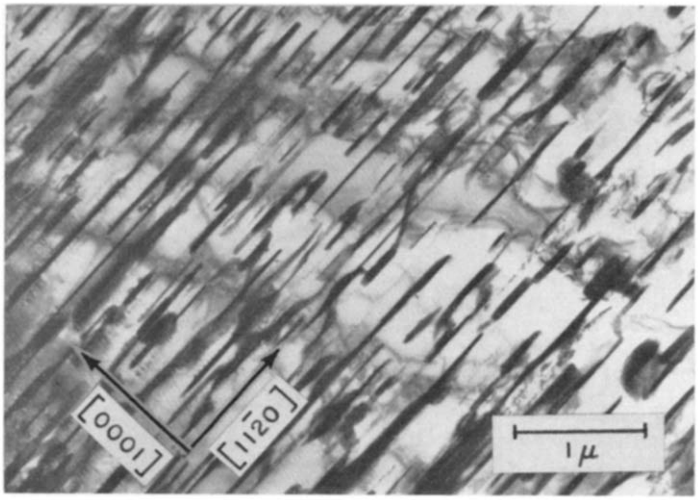

FIG. 4. $Mg_{17}Al_{12}$ plates lying in the basal plane of the matrix. Plane of foil is near prism plane. Note the wide interplate spacing. Alloy sample was aged for 500 hr at 175°C.

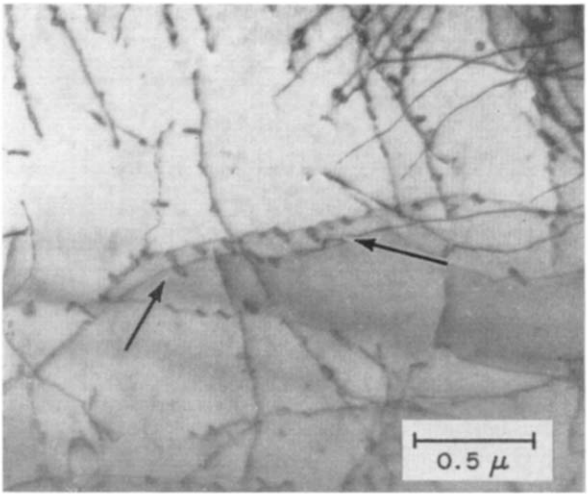

FIG. 5. Nucleation of $Mg_{17}Al_{12}$ plates on dislocations introduced prior to aging. Alloy sample was solution treated, strained 4%, and aged for 4 hr at 175°C. Plane of foil is near $(10\bar{1}1)$.

the electron microscope, dislocations were observed to be produced during growth of the $Mg_{17}Al_{12}$ plates. It is known that considerable expansion of these alloys occurs during precipitation.(2) These dislocations could thus be generated to relieve strain. They appeared—though not with great certainty—to form at the edges rather than at the broad faces of the plates.

The $Mg_{17}Al_{12}$ plates nucleate at dislocations (Fig. 5). Only a few dislocations are present in specimens quenched after the solution annealing treatment. Growth of $Mg_{17}Al_{12}$ plates, however, autocatalytically provides additional nucleation sites. Introduction of dislocations by cold work prior to aging markedly increases the density of precipitates for a given time of aging. However, nucleation occurs most rapidly in the interfaces of, and within, $\{10\bar{1}2\}$ twins as shown in Fig. 6. Note the very small amount of precipitate in the untwinned regions. This marked preference for precipitation within the $\{10\bar{1}2\}$ twins was seen also in Mg–Zn alloys.(1) Little is known concerning either the dislocation mechanisms for the formation of these twins or the structure of the twin interface; however, local rearrangement of the dislocations in the twin interface during the early times at the elevated aging temperature may produce local regions of disorder conducive to nucleation of precipitate. Also since the $\{10\bar{1}2\}$ twins are lenticular, the twin interface may consist of a series of steps, with local regions of disorder. A high density of dislocations also exists within the $\{10\bar{1}2\}$ twins, possibly producing the preferential nucleation observed within the twins away from the interface. In order of decreasing preference, nucleation in cold worked material occurs first at $\{10\bar{1}2\}$ twin interfaces, at grain boundaries, within the twins, and at dislocations in the untwinned matrix.

Even a small amount of cold work prior to aging markedly increases the rate of hardening. The striking effect of only 1% permanent tensile strain prior to aging is shown in Fig. 7. The time to reach an intermediate hardness is much reduced, especially at 150°C. However, the maximum hardness of the cold worked alloy does not exceed appreciably the limiting value of the conventionally aged material. Thus the 150°C aging curves merge after 450 hr. Larger amounts of prior strain produce similar results.

(b) *Cellular or discontinuous precipitation.* In Mg–Al alloys, cellular precipitation is not a low temperature process as in other systems,(10) but occurs simultaneously and competitively with the general precipitation over a wide temperature range. This is illustrated in Fig. 8 which shows the *C* curve for the start of cellular reaction. Cellular precipitation is arrested when general precipitation relieves the solute supersaturation in front of the advancing nodule. Cellular precipitation is most pronounced at temperatures near the knee of the *C* curve and, at 200°C, constitutes about 20% of the volume of the alloy. At other temperatures the proportion of cellular structure is smaller. As in other alloy systems,(11) the distribution of the cellular precipitate varies greatly from boundary to boundary. Electron diffraction indicated that the cellular precipitation forms at high angle or disordered grain boundaries.

Cellular precipitation in this Mg–Al alloy occurs by the mechanism developed by Smith,(12) i.e. a grain boundary migrates into the adjacent grain with

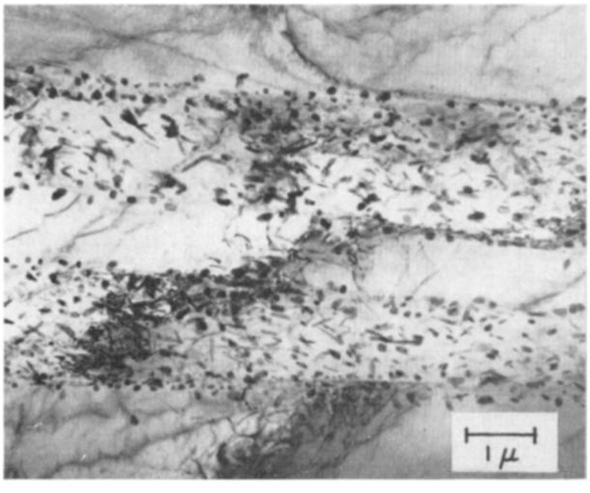

FIG. 6. Preferential precipitation of $Mg_{17}Al_{12}$ within $\{10\bar{1}2\}$ twins. Alloy sample was solution treated, strained 4%, and aged for 4 hr at 175°C.

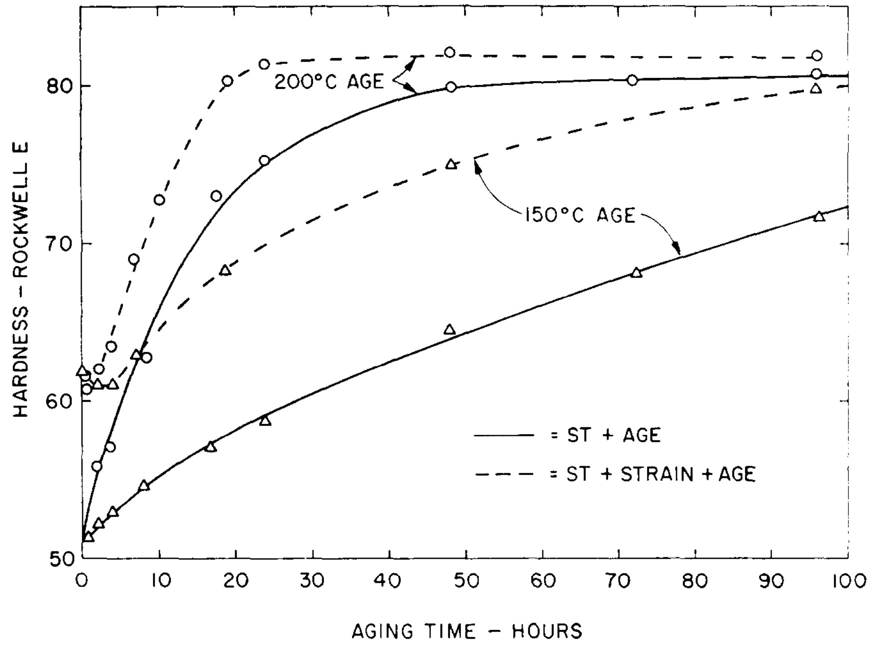

FIG. 7. The effect of prior cold work on the age hardening of a Mg–9 wt.% Al alloy. Prior strain—1% permanent tensile strain.

lamellae of precipitate and depleted matrix forming behind the advancing grain boundary. In this alloy, the earliest stage in the development of a cellular nodule is local instability of the grain boundary, as illustrated in Fig. 9. Between the anchoring grain boundary precipitates, the boundary begins to kink, i.e. to migrate locally. With continued aging, the local migration of the boundary continues until the boundary breaks away from the grain boundary precipitate and moves on a broad front into the adjacent grain as shown in Fig. 10. It is seen that this nodule has nucleated in the lower grain because the magnesium solid solution of the nodule is continuous with the lower grain. In this figure, the plane of the foil is nearly parallel to the basal plane of the lower grain. Note that the $Mg_{17}Al_{12}$ lamellae in the cellular nodule also form parallel to the basal plane of the nodule matrix. In all nodules observed, the $Mg_{17}Al_{12}$ lamellae formed parallel to the same habit plane of the magnesium solid solution matrix as the general

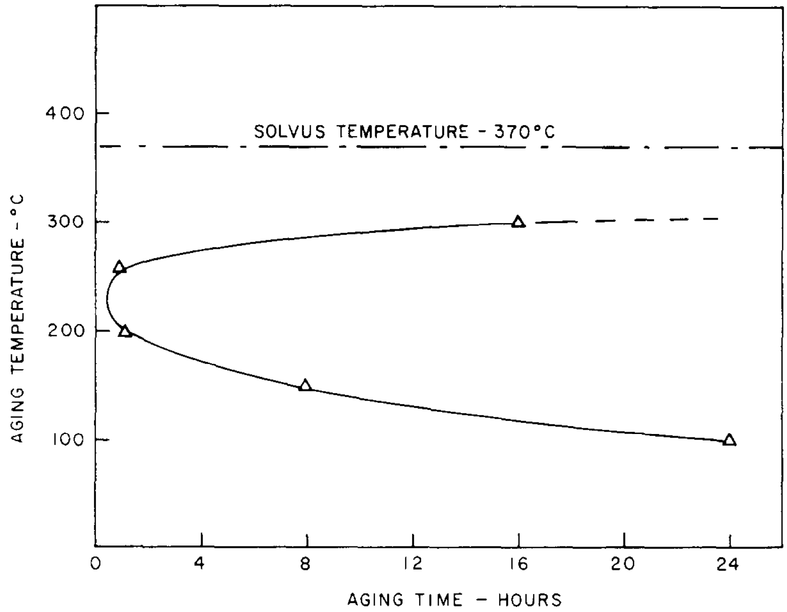

FIG. 8. The $C$ curve for the start of the cellular precipitation in a Mg–9 wt.% Al alloy as determined by light microscopy at ×50.

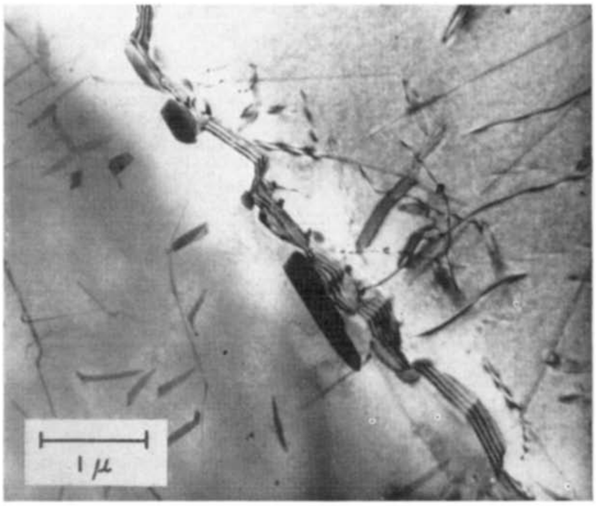

FIG. 9. The first stage of cellular precipitation—local migration of high-angled grain boundaries. The alloy sample was aged for 30 min at 260°C.

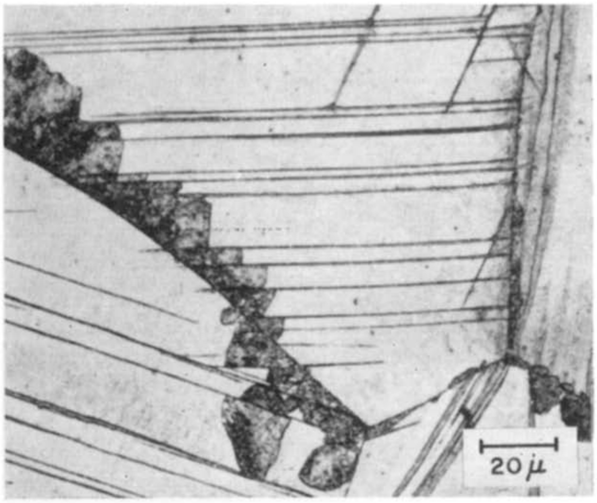

FIG. 11. The arrest of cellular nodule at {10$\bar{1}$2} twins introduced by a 6% cold roll prior to a 16 hr age at 150°C.

precipitate. Note, however, that the lateral growth on the habit plane is quite irregular. Thus when viewed from another orientation, the lamellar structure of the cellular nodules of this system appear quite ragged.

In Fig. 10 there appears to be a gap between the nodule interface and the $Mg_{17}Al_{12}$ lamellae. Actually, however, this is a projection effect produced by the nodule interface being at a shallow angle to the foil surface. In all cases, both phases of the nodules were in contact with the advancing nodule interface.

The ratio of cellular to general (intragranular) precipitation is reduced greatly by cold work prior to aging. Two factors are involved: first, increased nucleation on dislocations accelerates the general precipitation and results in more rapid relief of supersaturation, thus eliminating the driving force for the cellular precipitation; secondly, the prior cold work introduces {10$\bar{1}$2} twins in which general precipitation occurs very rapidly. These heavily precipitated twins act as barriers to nodule growth as illustrated in Fig. 11.

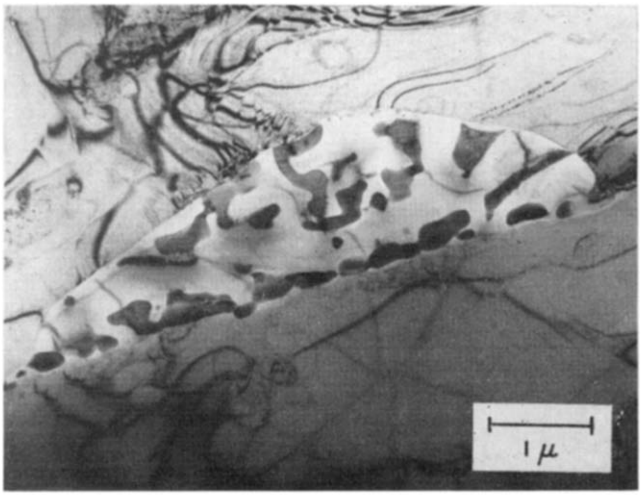

FIG. 10. A typical cellular nodule nucleated in the lower grain and growing into the upper grain. The basal plane of the lower grain is approximately parallel to the foil surface, thus the broad faces of the $Mg_{17}Al_{12}$ lamellae in the nodule are seen. The alloy sample was aged 6 hr at 175°C.

### *Age hardening mechanism*

In the solution treated condition, or in the presence of a small amount of precipitate, basal slip and {10$\bar{1}$2} twinning are the principal deformation modes. Slip dislocations move in planar arrays along the basal plane (see Fig. 12). In agreement with Hirsch and Lally,(13) under these conditions, the Burgers vectors of the dislocations are in the basal plane. These planar dislocations pile up at {10$\bar{1}$2} twin and grain boundaries as illustrated in Fig. 13.

As the amount of precipitate increases the nature of the deformation processes changes considerably. Cross slip occurs and {10$\bar{1}$2} twinning progressively disappears. The surfaces of two pre-polished specimens, one on the solution treated condition and the other aged to full hardness (24 hr at 260°C) after a 4% compression strain at room temperature, are compared in Fig. 14. The slip traces were analyzed in several grains in each specimen. In Fig. 14(A), fine basal slip and wide lenticular {10$\bar{1}$2} twins are seen. In Fig. 14(B) there is a near absence of twins and a second slip system is now operative. In age hardened specimens,

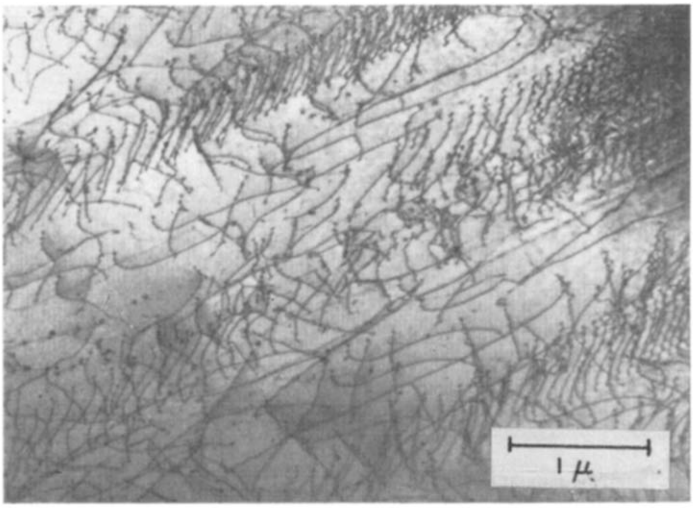

Fig. 12. Arrays of dislocations in the basal plane. The alloy sample was strained 4% in the solution treated condition, then aged for 4 hr at 175°C. Nucleation of $Mg_{17}Al_{12}$ plates on the dislocations is evident. Plane of foil—$(21\bar{3}1)$. Operating reflections $(\bar{1}101)$ and $(02\bar{2}2)$.

in which the second slip system is not always as well defined as in Fig. 14(B), replication electron microscopy shows that the fine basal slip lines seen in the solution treated specimens [Fig. 15(A)] have been replaced by wavy slip (Fig. 15B). Reed-Hill and Robertson(14) also found that prismatic slip occurs at room and lower temperatures in pure magnesium single crystals oriented so as to block basal slip and $\{10\bar{1}2\}$ twinning. In the aged Mg–Al alloys, basal slip and $\{10\bar{1}2\}$ twinning are suppressed by precipitation rather than by a matrix orientation effect.

In heavily precipitated specimens, cross slip on the prism planes generates complex dislocation tangles (Fig. 16). As the size and number of $Mg_{17}Al_{12}$ plates increases, the areas of planar arrays of basal dislocations decrease and the areas of complex tangles increase. Thus, it would appear that the $Mg_{17}Al_{12}$ plates give rise to prismatic slip which, combined with basal slip, produces complex dislocation tangles which harden the alloy.

Unlike twins in Mg-Zn alloys,(1) the $\{10\bar{1}2\}$ twins in the Mg–Al alloys do not shear the $Mg_{17}Al_{12}$ plates. Perhaps because the $Mg_{17}Al_{12}$ plates are much larger than the thin MgZn′ laths of Mg–Zn alloys. As the size and the number of $Mg_{17}Al_{12}$ plates increase the amount of $\{10\bar{1}2\}$ twinning proportionately decreases.

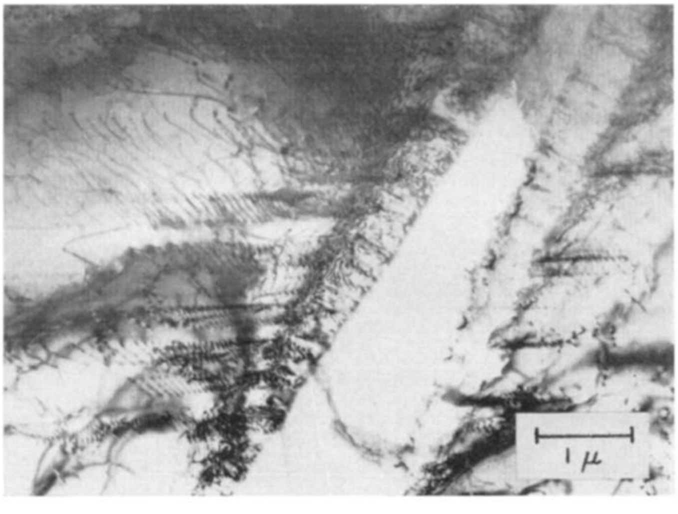

Fig. 13. The pile up of dislocations at a $\{10\bar{1}2\}$ twin boundary. Structure of twin is out of contrast. Plane of foil parallel to $(02\bar{2}1)$ of matrix. Several reflections are operating.

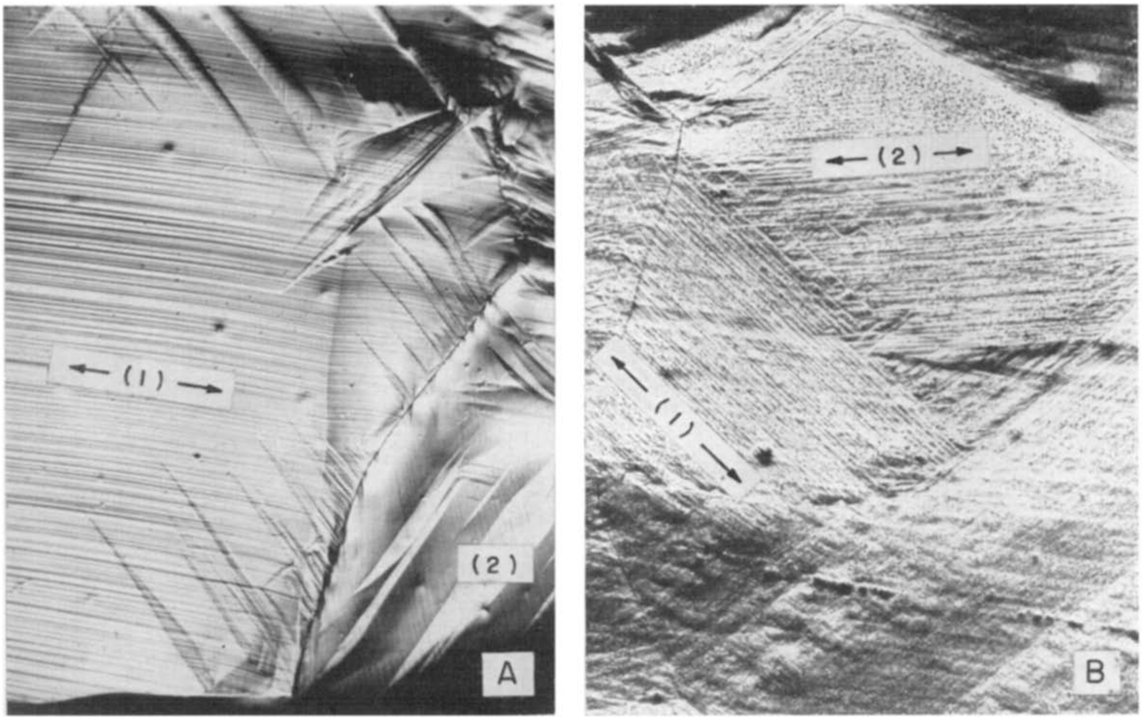

(A) Solution treated condition + strain.

Basal slip (1) and {10$\bar{1}$2} twins (2) are principal deformation mechanisms. Alloy specimen was solution treated, the surface chemically polished and strained 4% in compression.

(B) Fully age hardened condition + strain.

Basal slip (1) and prismatic slip (2) predominate. {10$\bar{1}$2} twins are almost completely absent. Alloy specimen was solution treated, the surface chemically polished, then aged for 24 hr at 260°C, and strained 4% in compression.

FIG. 14. The effect of precipitation on the room temperature deformation processes of a Mg–9 wt.% Al alloy. ×150

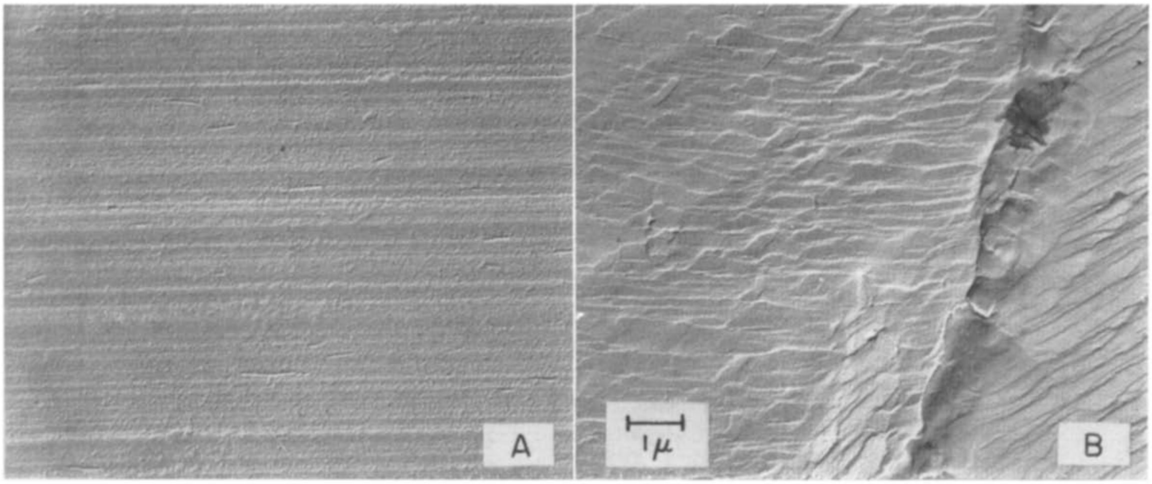

(A) Fine basal slip in a solution treated specimen.

(B) Wavy slip in a fully age hardened specimen (16 hr at 260°C).

FIG. 15. The effect of precipitation on the fine structure of slip traces as seen by electron replication microscopy.

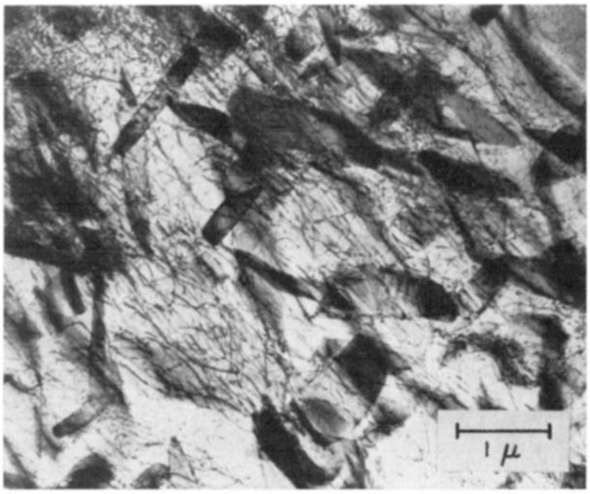

FIG. 16. Dislocation tangles in a heavily precipitated Mg–9 wt.% Al alloy (aged 4 hr at 260°C + 4% tensile strain). Plane of foil is $(0\bar{1}11)$, several reflections are operating.

However, $\{10\bar{1}2\}$ twinning never fully disappears even after apparently complete suppression. For example, electron diffraction of the structure of Fig. 16 shows a few faint twin spots, indicating that a few areas of the heavily worked matrix are in the twin orientation even though no twins are resolvable. The mechanism by which precipitation suppresses twin formation is still uncertain. However, since the twin does not shear the $Mg_{17}Al_{12}$ plates, the plates provide resistance to twin growth in that the twin must envelop the plate by transforming the matrix around it. This enveloping process is sometimes not completed and as shown in Fig. 17, steps are seen in the twin-matrix interface as though the thickening of the twin was retarded by the $Mg_{17}Al_{12}$ plate. With increasing amount of precipitate, growth of the twins is progressively inhibited until they are finally unable to grow to resolvable size.

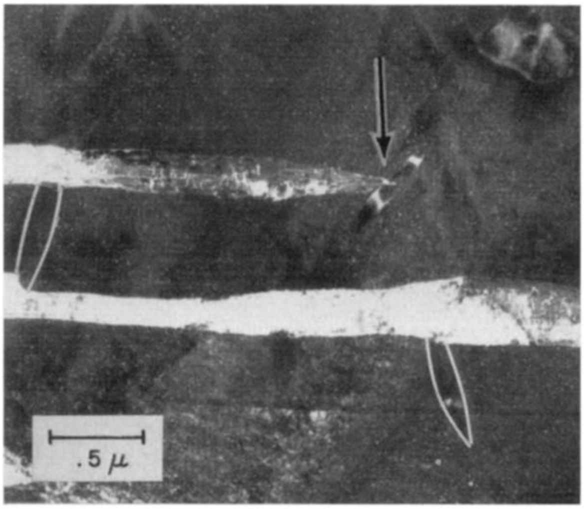

FIG. 17. Dark field image showing discontinuities of $\{10\bar{1}2\}$ twin boundaries at intersections with $Mg_{17}Al_{12}$ plates in an aged and deformed alloy sample. Some of the $Mg_{17}Al_{12}$ plates are outlined for clarity. At the arrow, a $\{10\bar{1}2\}$ twin impinges on a $Mg_{17}Al_{12}$ plate. Plane of the foil is near $(\bar{1}100)$ of alloy matrix and the (0001) of the twins. The $(10\bar{1}0)$ reflection of the twin was selected for the dark field image. Alloy sample was aged 2 hr at 260°C; then deformed.

The deformation modes for a given precipitate dispersion remain essentially unchanged over the temperature range from 25°C to −196°C. No new slip systems were activated. Consequently, the temperature dependence of the flow stress was small as shown in Fig. 18.

## DISCUSSION

In view of the simple precipitation process in Mg–Al alloys, it is not suprising that the age hardening response of these alloys is small. In general, the precipitation of a transition lattice, much less an equilibrium phase, does not produce an inter-plate spacing small enough to require shearing of the precipitate for dislocation motion and thus a large increase in strength. Prior cold work of Mg–Al alloys does introduce additional nucleation sites for the $Mg_{17}Al_{12}$ precipitate (in the form of dislocations), and the interplate spacing is somewhat reduced. But the resulting interplate distances are never sufficiently small to require shearing of the $Mg_{17}Al_{12}$ plates. In Mg–Al alloys, the role of the $Mg_{17}Al_{12}$ precipitate is to break up basal glide, cause cross slip and thus produce dislocation tangles which, in effect, strain harden the matrix. Although strain hardening is effective in h.c.p. alloys, and many commercial magnesium alloys derive their properties from controlled strain hardening, the increased strength thus produced is not as large as in systems such as Al–Cu, in which shearing of the G.P. zones, the hardening structure, is required for dislocation motion.

In the Mg–Al and Mg–Zn alloy systems, there appears to be no inherent property of the h.c.p. matrix which produces the poor age hardening response of these systems. Rather the small degree of hardening derives from the basic characteristics of the precipitation processes of each alloy system. The precipitation processes of these alloys are compared in Table 1. It is seen that, although the precipitation processes are quite different, both have characteristics which produce poor hardening. In the Mg–Zn system, although the MgZn′, the hardening precipitate, is efficiently oriented to block basal slip, the solubility of

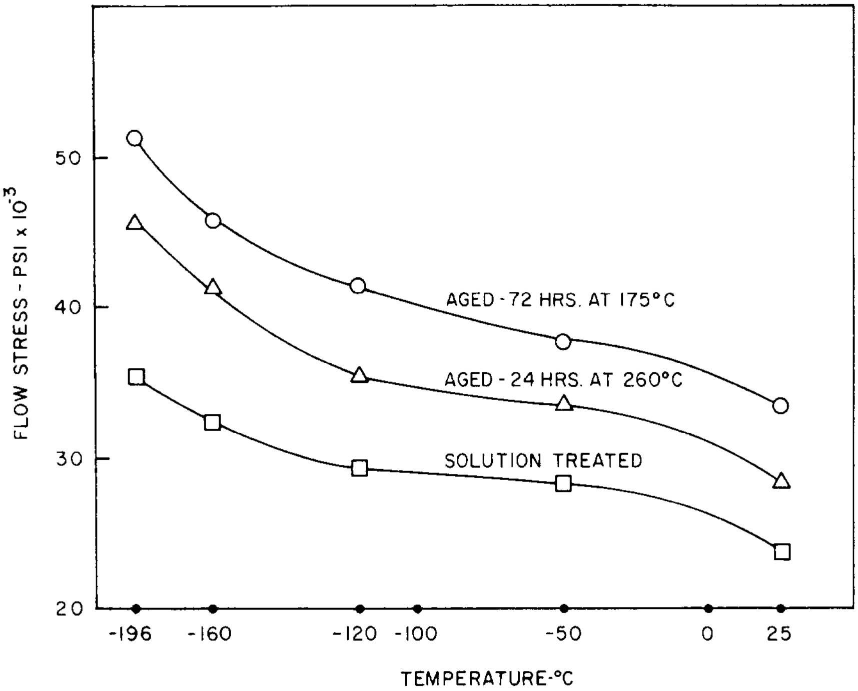

FIG. 18. Temperature dependence of the flow stress of Mg–9 wt.% Al alloy.

TABLE 1. Comparison of precipitation and deformation characteristics of Mg–Al and Mg–Zn alloys

| | Mg–Al | Mg–Zn |
|---|---|---|
| Hardening precipitate | Equil. phase–$Mg_{17}Al_{12}$ | Transition lattice–MgZn′ |
| Structure | α-Mn–Complex cubic | $MgZn_2$–Laves phase |
| Habit plane | Basal | Prism |
| Morphology | Plates | Laths |
| Slip–precipitate interaction | Cross slip and tangling of dislocations | Orowan-dislocations bow between MgZn′ laths |
| Twin–precipitate interaction | $\{10\bar{1}2\}$ Twins suppressed | $\{10\bar{1}2\}$ Twins shear MgZn′ laths |

zinc in magnesium (on a volume basis) is too low to produce a fine dispersion of MgZn′; also, $\{10\bar{1}2\}$ twinning is always available. In the Mg–Al system, although $\{10\bar{1}2\}$ twinning is suppressed and the solubility of aluminum in magnesium is larger, the $Mg_{17}Al_{12}$ plates are not oriented to block basal slip effectively and, more importantly, the precipitate size and inter-plate spacing are always large. The alloys of both these systems are age hardened by precipitates which require heterogeneous nucleation. Until the inter-particle spacing of these hardening precipitates can be reduced, possibly by a process which will produce a finer dispersion of nucleation sites, strain hardening rather than precipitation hardening is the best method for improving the strength properties of these alloys.

## ACKNOWLEDGMENTS

The author is indebted to L. Sturkey of the Dow Metal Products Company for helpful discussions and to H. I. Aaronson for review of the manuscript. Thanks are also due to C. J. Amberger for the development of thinning procedures for the aged Mg–Al alloy and for preparation of the foils for the electron microscope.

## REFERENCES

1. J. B. Clark, *Acta Met.* **13**, 1281 (1965).
2. A. M. Talbot and J. T. Norton, *Trans. Am. Inst. Min. Engrs* **122**, 301 (1936).
3. W. Bulian and E. Fahrenhorst, *Z. Metallk.* **34**, 285 (1942).
4. F. A. Fox and E. Lardner, *J. Inst. Metals* **69**, 373 (1943).
5. T. E. Leontis and C. E. Nelson, *Trans. Am. Inst. Min. Engrs* **191**, 120 (1951).
6. Y. Murakami, O. Kawano and H. Tamura, *Mem. Fac. Engng Kyoto Univ.* **24**, Part 4, 411 (1962).
7. P. M. Kelly and J. Nutting, *J. Inst. Metals* **87**, 385 (1958–59).
8. H. I. Aaronson, *Decomposition of Austenite by Diffusional Processes*, edited by V. F. Zackay and H. I. Aaronson, p. 462. Interscience (1962).
9. J. B. Clark, *High Temperature, High Resolution Metallography*, edited by H. I. Aaronson and G. S. Ansell. Gordon & Breach (1967).
10. H. Böhm, *Z. Metallk.* **52**, 564 (1961).
11. W. Gruhl and D. Ammann, *Acta Met.* **3**, 347 (1955).

12. C. S. Smith, *Trans. Am. Soc. Metals* **45,** 533 (1953).
13. P. B. Hirsch and J. S. Lally, *Phil. Mag.* **12,** 595 (1965).
14. R. E. Reed-Hill and W. D. Robertson, *Trans. Am. Inst. Min. Engrs* **209,** 496 (1957).

## APPENDIX

### *Preparation of Thin Foils of Mg–9 wt.% Al Alloy by the Window Method*

This chemical thinning procedure is recommended for heavily precipitated Mg–Al alloys only.

*Solutions*

1. Thinning solution: Concentrated *ortho*-phosphoric acid (85% $H_3PO_4$) maintained between 20–80°C.
2. Rinse solution: Pure ethyl alcohol.
3. Dip-rinse solution: 20 g anhydrous citric acid dissolved into 500 ml of pure ethyl alcohol.
4. Final rinse: Pure ethyl alcohol.

Solutions 1 and 2 are agitated by magnetic stirrers. The rate of stirring is adjusted to form a moderate vortex.

*Procedure*

A. Immerse masked foil completely into a 250 ml beaker of $H_3PO_4$ (Solution No. 1), allowing the foil to swirl freely in solution until half the window is consumed. 90 min are required for a solution temperature of 20°C; 10–15 min for solution temperature of 70–80°C with foils initially 0.006 in. thick.

B. Transfer the foil to a 250 ml beaker of agitating pure ethyl alcohol (Solution No. 2) by means of non-metallic forceps, and hold the foil submerged until all attack by the phosphoric acid has ceased.

C. Transfer the foil from the ethyl alcohol rinse to a beaker filled with the citric acid dip-rinse (Solution No. 3) and agitate for 4–6 sec.

D. Transfer the foil to a pure ethyl alcohol rinse (Solution No. 4), agitate for 10 sec or more, then immediately dry the foil between filter papers.